CARBON CYCLING

Bomb radiocarbon evidence for strong global carbon uptake and turnover in terrestrial vegetation

Heather D. Graven[1]*, Hamish Warren[1], Holly K. Gibbs[2], Samar Khatiwala[3], Charles Koven[4], Joanna Lester[1], Ingeborg Levin[5]†, Seth A. Spawn-Lee[6,7], Will Wieder[8]

Vegetation and soils are taking up approximately 30% of anthropogenic carbon dioxide emissions because of small imbalances in large gross carbon exchanges from productivity and turnover that are poorly constrained. We combined a new budget of radiocarbon produced by nuclear bomb testing in the 1960s with model simulations to evaluate carbon cycling in terrestrial vegetation. We found that most state-of-the-art vegetation models used in the Coupled Model Intercomparison Project underestimated the radiocarbon accumulation in vegetation biomass. Our findings, combined with constraints on vegetation carbon stocks and productivity trends, imply that net primary productivity is likely at least 80 petagrams of carbon per year presently, compared with the 43 to 76 petagrams per year predicted by current models. Storage of anthropogenic carbon in terrestrial vegetation is likely more short-lived and vulnerable than previously predicted.

The processes contributing to the net sink of CO_2 in the terrestrial biosphere are not yet well understood and will likely change in the future (*1*), making it difficult to predict future climate change and create effective mitigation and adaptation policies. Future climate predictions require robust representation of the global carbon cycle, which is challenging when basic properties still have large uncertainties. In particular, observational constraints on global net primary productivity (NPP), the rate of creation of new plant tissues and products, and on carbon turnover rates are lacking. Estimates of global NPP rely on statistical or model-based estimates that use site-scale data (*2*); however, it is very difficult to measure all components of NPP (*3*), and there are not many sites with comprehensive measurements, especially in the tropics (*4*). A large range of global NPP of 43 to 76 petagrams of carbon (PgC) per year is currently simulated by models (*5*, *6*), and these models do not generally show a strong trend over the 20th century. This is in contrast to the trend found for gross primary productivity (GPP) (+30%) (*7*), which is typically twice as large as NPP. Here, we provide global-scale constraints on NPP and carbon turnover by analyzing radiocarbon (^{14}C) produced by nuclear bomb testing and models of the terrestrial biosphere and vegetation.

[1]Department of Physics, Imperial College London, London, UK. [2]Nelson Institute for Environmental Studies and the Department of Geography, University of Wisconsin-Madison, Madison, WI, USA. [3]Department of Earth Sciences, University of Oxford, Oxford, UK. [4]Climate and Ecosystem Sciences Division, Lawrence Berkeley National Laboratory, Berkeley, CA, USA. [5]Institute of Environmental Physics, Heidelberg University, Heidelberg, Germany. [6]Department of Integrative Biology, University of Wisconsin-Madison, Madison, WI, USA. [7]The Nature Conservancy, Arlington, VA, USA. [8]Climate & Global Dynamics, National Center for Atmospheric Research, and Institute of Arctic and Alpine Research, University of Colorado, Boulder, CO, USA.
*Corresponding author. Email: h.graven@imperial.ac.uk
†Deceased.

Global bomb radiocarbon budget

Nuclear bomb testing in the 1950s and 1960s produced excess ^{14}C in the atmosphere (Fig. 1A), which was assimilated into the terrestrial biosphere and ocean through photosynthesis and air-sea gas exchange over time. Tracking how ^{14}C accumulated in the terrestrial biosphere after the bomb testing can therefore enable evaluation of the rates of carbon uptake and turnover (*8*). However, the global accumulation of ^{14}C in the biosphere cannot be observed directly; from new leaves to highly aged soil carbon, there is too much heterogeneity in ^{14}C content in the biosphere.

We use a budgeting approach to diagnose the ^{14}C accumulation in the terrestrial biosphere caused by bomb testing to evaluate carbon cycling in terrestrial biosphere models. In this approach, the ^{14}C accumulation in the terrestrial biosphere is calculated using observations in the stratosphere and troposphere and observationally constrained ocean models to close the ^{14}C budget. In contrast to prior work (*9*) that examined the period from 1945 to 2005, we focus here on the period 1963 to 1967, when atmospheric ^{14}C was highly elevated relative to the biosphere but no strong detonations took place (green area in Fig. 1A) (*10*). Therefore, total ^{14}C in the Earth system was roughly constant but exchanged between reservoirs over 1963 to 1967. This allows us to focus on the period when there was good observational coverage of the stratosphere by aircraft and balloon sampling and to avoid uncertainty and assumptions with calculating the total ^{14}C produced by the bombs and estimating the pre-bomb ^{14}C content. Another advantage of focusing on 1963 to 1967 is that we sharpen the constraint on ^{14}C uptake and turnover in vegetation, where the ^{14}C first entered the terrestrial biosphere, before much ^{14}C was transferred to litter and soil pools.

We used stratospheric data originally published in reports of the Health and Safety Laboratories, which were reassessed and r
culated with corrected standard values (*11*
and used in an atmospheric model to calculate global stratospheric ^{14}C inventories (*12*) (Fig. 1). Tropospheric ^{14}C inventories were calculated from global compilations recently produced for modeling purposes (*14*, *15*). Ocean ^{14}C simulations (*16*–*19*) that match revised ocean ^{14}C inventories (*20*, *21*) from the 1970s (GEOSECS) and 1990s (WOCE) were used for ocean ^{14}C inventories.

After the ^{14}C was initially deposited in the stratosphere, the stratosphere lost ~200×10^{26} atoms of ^{14}C through mixing of the ^{14}C into the troposphere over 1963 to 1967, which experienced a net gain of about 40×10^{26} atoms. The ocean gained about 80×10^{26} atoms through air-sea exchange (Fig. 1B). We estimate that the terrestrial biosphere therefore must have accumulated $86 \pm 18 \times 10^{26}$ atoms [95% confidence interval (CI)] (*22*) over 1963 to 1967 (Fig. 1C) as the assimilation of ^{14}C outpaced the turnover of ^{14}C back to the air.

Terrestrial biospheric ^{14}C accumulation in the CESM2 model

The terrestrial biospheric ^{14}C accumulation over 1963 to 1967 provides a new constraint on coupled climate-carbon cycle models (also known as Earth system models or ESMs), which are used to inform global climate policy but have particularly uncertain terrestrial carbon cycle components because of the heterogeneity and complexity of land ecosystems. Simulations of the only such land model to simulate ^{14}C explicitly within an ESM, the Community Land Model version 5.0 (CLM5.0) (*23*), accumulate a much lower amount of ^{14}C in the terrestrial biosphere (~40×10^{26} atoms) than our observation-based estimate ($86 \pm 18 \times 10^{26}$ atoms; Fig. 1C). Simulations of CLM5.0 driven with observed climate data (CLM5.0-unc, where "unc" means "uncoupled") (*24*) and coupled model simulations of the Community Earth System Model 2 (*25*) Large Ensemble Project (CESM2-LENS) (*26*, *27*) following the Coupled Model Intercomparison Project (CMIP) phase 6 historical (concentration-driven) simulation protocol show similar ^{14}C accumulation, and the spread across nine ensemble members is small (Fig. 1C). CLM5.0-unc results are similar to another offline simulation of CLM5.0 that suggested the ^{14}C accumulated in the terrestrial biosphere in the 1960s could be too small (*28*).

In 1963 to 1967, not much bomb ^{14}C had yet entered the soil, as most biospheric bomb ^{14}C was in vegetation (Fig. 1C). In CESM2-LENS, 56% of the ^{14}C accumulated in vegetation, with only 18% in litter and coarse woody debris and 26% in soils over 1963 to 1967. If the ^{14}C accumulation in vegetation in CESM2 were correct, then the ^{14}C accumulation in nonvegetation pools would have to be >3 times larger than simulated in CESM2-LENS and >75% of the total

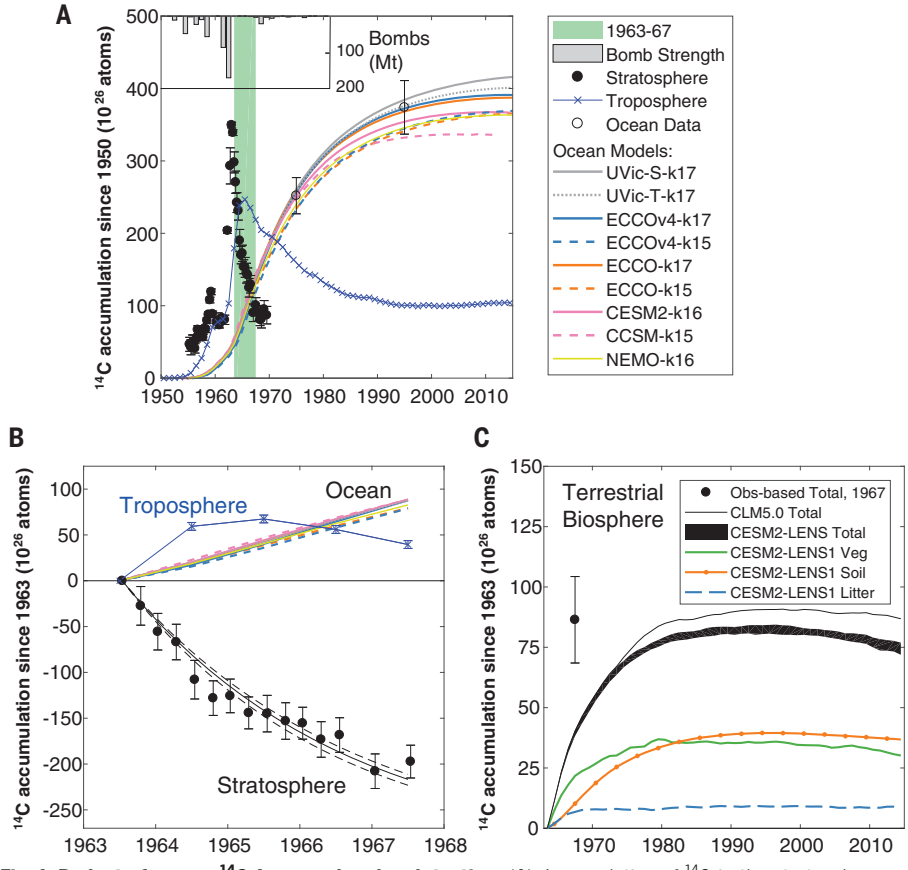

Fig. 1. Budget of excess ^{14}C from nuclear bomb testing. (**A**) Accumulation of ^{14}C in the stratosphere (*12*), troposphere (*14*, *15*), and ocean since 1950 based on observations and simulated accumulation of ^{14}C in ocean models (*16*–*18*) selected to match observations (*20*, *21*) in the 1970s and 1990s. Inset shows annual nuclear bomb strength in units of megatons of TNT equivalents (*10*). The period 1963 to 1967 with no strong nuclear detonations is highlighted in green. (**B**) ^{14}C accumulation in the stratosphere, troposphere, and ocean since 1963 focusing on the period 1963 to 1967 [green area in (A)]. The black solid line shows an exponential fit to the stratospheric data, and the dashed lines show the 1-σ uncertainty in the χ^2 fit. (**C**) Our new observation-based estimate of ^{14}C accumulation in the terrestrial biosphere in 1967 relative to 1963 (black circle) based on the budgeting approach and simulations of the CLM5.0 model driven with observed climate data (CLM5.0-unc) or as part of CESM2-LENS. The black area shows the range of ^{14}C accumulation in the terrestrial biosphere across nine ensemble members. ^{14}C accumulation in vegetation, soils, and litter (including coarse woody debris) are shown for CESM2-LENS ensemble member 1001.001.

^{14}C accumulation to match the observation-based estimate. It is unlikely that more than half of the biospheric ^{14}C accumulation over 1963 to 1967 occurred in dead plant material and soils because the peak in global mean tropospheric ^{14}C occurred only in 1964–1965.

We thus conclude that the ^{14}C accumulation in vegetation over 1963 to 1967 in CESM2 is too low (Fig. 1). The underestimate for vegetation could be because the NPP in the model is too low, so not enough ^{14}C enters the vegetation, and/or because carbon is misallocated between short-lived versus long-lived pools, so ^{14}C is turned over too quickly.

Vegetation model emulators and model-data comparisons

CESM2 is the only Earth system model with explicit simulations of ^{14}C available. Therefore, to simulate the ^{14}C accumulation in other models and to explore the sensitivity of the ^{14}C accumulation to NPP and carbon stocks, we needed to construct emulator models. We found that the variables included in CMIP were not sufficient to construct a reliable emulator model for the whole terrestrial biosphere for CESM2, but ^{14}C in vegetation could be modeled reliably (Figs. 2 to 4).

We focus now on analyzing the ^{14}C accumulation only in vegetation in models over 1963 to 1967. We constructed a simple emulator model for woody (long-lived: stem and coarse roots) and nonwoody (short-lived: leaves, fine roots, and other pools) vegetation biomass run on each model grid cell (*22*). We applied the emulator model to CESM2-LENS member 1001.001 and to models from CMIP5 and CMIP6 that reported the necessary variables. We examined global sums for woody and nonwoody pools across all biomes and grid cells (Figs. 2 to 4 and fig. S1), so the global nonwoody vegetation biomass includes the nonwoody vegetation biomass in forests as well as other biomes. We compared these with satellite-based vegetation carbon products (*29*–*31*) that omit leaf carbon in forests, so we estimated global total leaf carbon in forests to be 14.3 PgC [based on table S5 in (*32*)] and added this to the observation-based estimates of vegetation carbon stocks.

To evaluate the vegetation ^{14}C simulations, we estimated the true ^{14}C accumulation in vegetation by subtracting the ^{14}C accumulation in litter, coarse woody debris, and soils simulated by CESM2-LENS member 1001.001 from the observation-based total terrestrial biosphere ^{14}C accumulation over 1963 to 1967. We allowed the uncertainty in nonvegetation ^{14}C accumulation to be ±100% (95% CI) (*22*), even though CESM2/CLM5 is in fact likely to overestimate this ^{14}C accumulation because its proportion of fresh carbon in both surface and subsurface soils has been shown to be too high (*33*). Our estimate of vegetation ^{14}C accumulation is 69 ± 24 $\times 10^{26}$ atoms (95% CI) over 1963 to 1967, which allows for a possible range of 43 to 100% of biospheric ^{14}C accumulation in vegetation.

Most of the CMIP5 and CMIP6 vegetation emulator models (five of seven) underestimate the observation-based vegetation ^{14}C accumulation over 1963 to 1967 (Fig. 2). The two models that match the observation-based vegetation ^{14}C accumulation have high NPP of >68 PgC/yr in 1965 (Fig. 2B, fig. S1, and table S1). One of the two models is from CMIP5 (IPSL5), whereas the CMIP6 version of that model (IPSL6) has much lower NPP and underestimates the observation-based vegetation bomb ^{14}C inventory. The other model matching the observation-based vegetation bomb ^{14}C inventory, CanESM5 from CMIP6, has high NPP and allocates a large fraction of its NPP to wood (68% in 1965), in contrast to other models allocating 22 to 43% of NPP to wood (table S1).

Overall, the ^{14}C accumulation in vegetation over 1963 to 1967 shows a strong relationship with NPP but not with vegetation carbon stock (Fig. 2). This indicates that higher NPP increases ^{14}C accumulation in vegetation over 1963 to 1967, but higher carbon stock (and slower turnover rate) generally does not. Two versions of the MRI model lie below a regression line between ^{14}C accumulation in vegetation and NPP for the other five models (Fig. 2B). The MRI models allocate the highest fraction of NPP to nonwoody vegetation (76 to 78% to nonwoody and 22 to 24% to woody), and their nonwoody annual NPP is similar to their nonwoody carbon stock (table S1), which indicates a very high level of productivity per unit

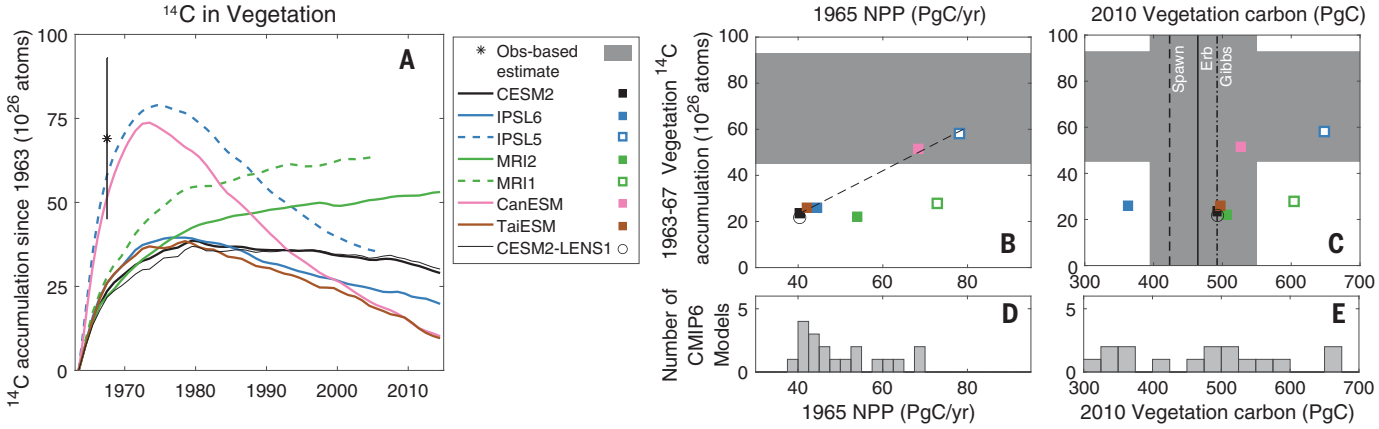

Fig. 2. Model-data comparison for vegetation in the emulator models and in CESM2. (**A**) Simulated accumulation of ^{14}C in vegetation since 1963 compared with the observation-based estimate of ^{14}C accumulation in vegetation over 1963 to 1967. (**B**) Accumulation of ^{14}C in vegetation over 1963 to 1967 versus NPP in 1965 in each emulator model and CESM2, including a regression line for emulator models excluding MRI models. Gray area shows the uncertainty range in the observation-based estimate of ^{14}C accumulation. (**C**) Accumulation of ^{14}C in vegetation over 1963 to 1967 versus carbon stock in vegetation in 2010 (2005 for MRI1 and IPSL5) in each emulator model and CESM2, including observation-based estimates of vegetation carbon stock (*29*–*31*). The gray area reflects the uncertainty from Erb *et al*. (*31*) and uncertainty in ^{14}C accumulation. (**D** and **E**) Histograms of NPP in 1965 and carbon stock in vegetation in 2010 in CMIP6 models, including additional models that could not be included in the vegetation emulator simulations because the available CMIP6 output for these models lacked the necessary variables to run the emulator model (table S2). The explicit simulation of ^{14}C in vegetation in CESM2-LENS member 1001.001 (CESM2-LENS1) is shown in (A) to (C) for comparison with the CESM2 vegetation emulator model.

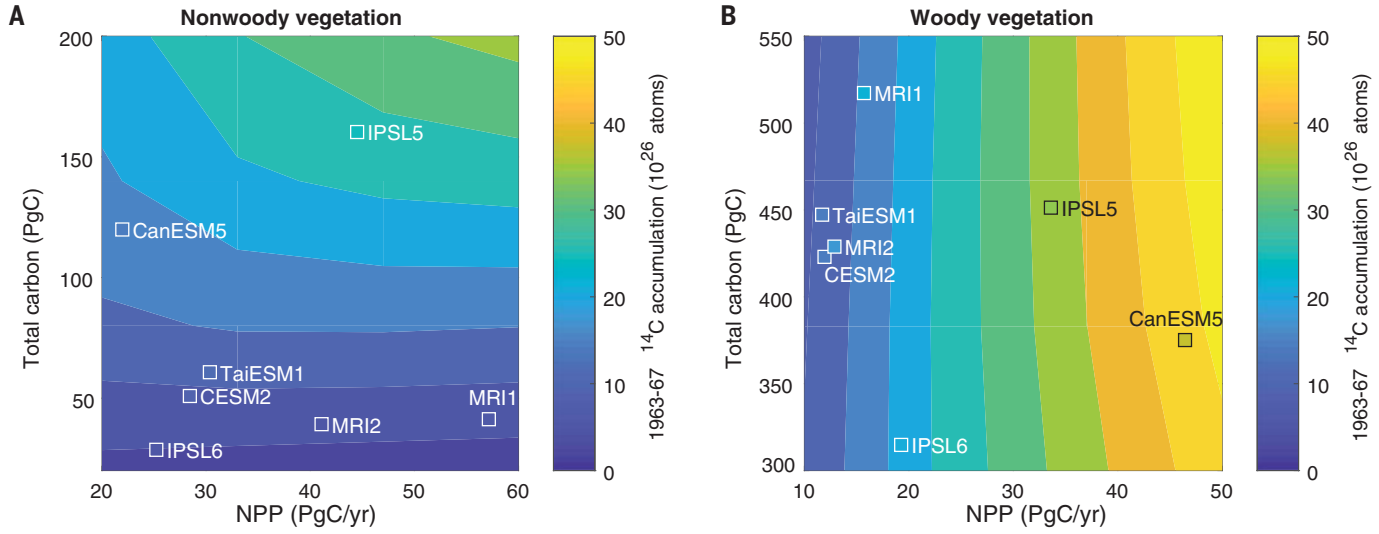

Fig. 3. Sensitivity of ^{14}C accumulation to NPP and total carbon. Accumulation of ^{14}C over 1963 to 1967 in nonwoody (**A**) and woody (**B**) vegetation biomass plotted in color with NPP and total carbon stock in 1965 on the *x* and *y* axes. Contours reflect relationships across 16 simulations of the CESM2 emulator, where NPP and total carbon stock were scaled across the range shown here. Symbols show ^{14}C accumulation in the emulator models using the same color bar.

biomass and a fast turnover rate. Therefore, the flux of ^{14}C into nonwoody vegetation in the MRI models is large but is turned over quickly, and the ^{14}C accumulation in nonwoody vegetation is among the lowest (Fig. 3A).

There are differing controls on ^{14}C accumulation over 1963 to 1967 in nonwoody versus woody vegetation biomass in the emulator models (Fig. 3 and figs. S2 and S3). Accumulation of ^{14}C in longer-lived woody vegetation is sensitive to NPP, whereas accumulation of ^{14}C in shorter-lived nonwoody vegetation is more sensitive to the carbon stock. At higher stocks of nonwoody vegetation carbon, ^{14}C accumulation in nonwoody vegetation is also sensitive to NPP. The patterns found for scaling experiments in the CESM2 vegetation emulator (contours in Fig. 3) are similar to the patterns found for the other vegetation model emulators (colored symbols in Fig. 3).

The patterns in Fig. 3 indicate that underestimated ^{14}C accumulation in vegetation over 1963 to 1967 is due to underestimated NPP or underestimated nonwoody vegetation biomass in models. Only IPSL6 underestimates the total vegetation carbon stock estimated with satellite data (Fig. 2C and fig. S4), so increasing nonwoody carbon stock in the models requires that carbon shifts from woody biomass (stems and coarse roots) to nonwoody biomass (leaves, fine roots, and other biomass) by adjustment of their turnover rates. The models tend to underestimate belowground vegetation

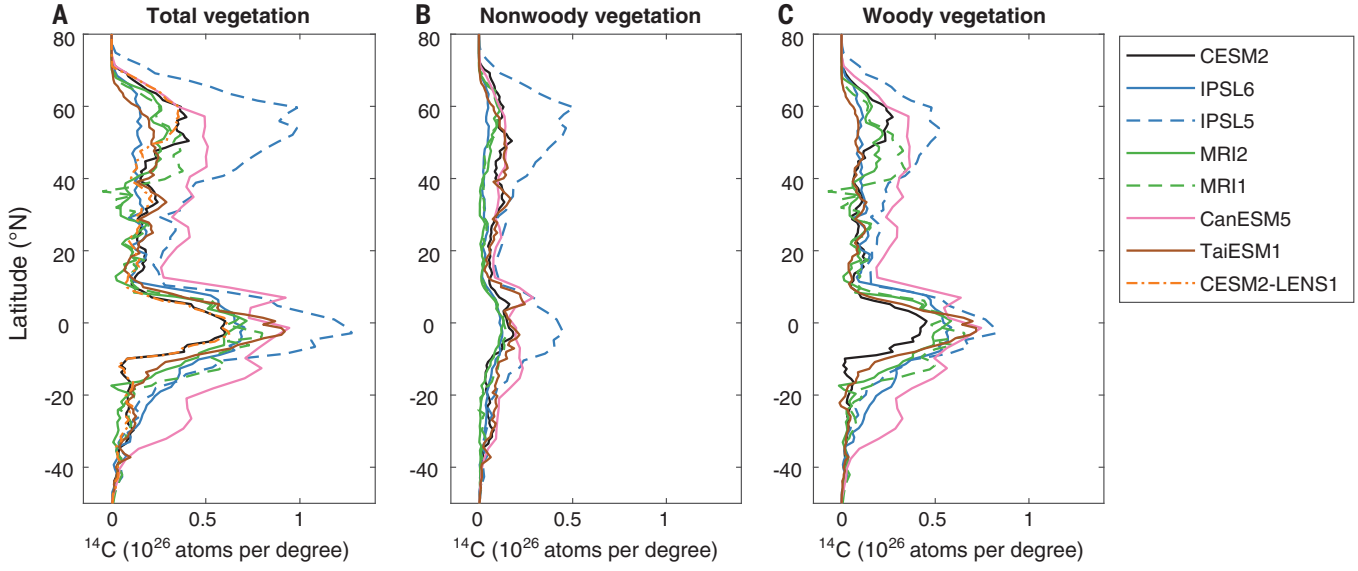

Fig. 4. Spatial distribution of ^{14}C accumulation simulated in vegetation in the emulator models and in CESM2. Accumulation of ^{14}C over 1963 to 1967 per degree latitude in total (**A**), nonwoody (**B**), and woody (**C**) vegetation biomass integrated over all longitudes. The explicit simulation of ^{14}C in CESM2-LENS1 is shown in (A) for comparison with the CESM2 emulator model.

carbon stocks (*29*, *30*) (fig. S5), so shifting aboveground woody carbon (stems) to belowground nonwoody carbon (fine roots) may be required. Conversely, NPP in woody (or nonwoody) vegetation could be increased in the models without necessarily affecting carbon stocks if modeled turnover rates are simultaneously increased.

The regression between vegetation ^{14}C accumulation and NPP (R^2 > 0.99), excluding the MRI models that have very high nonwoody NPP, suggests that NPP in 1965 should have been at least 63 PgC per year (the value of NPP at the intersection of the regression line and ^{14}C accumulation uncertainty range in Fig. 2B). However, only 16% of all CMIP6 models have NPP higher than 63 PgC per year in 1965 (Fig. 2D and table S2). Considering that total carbon assimilation (GPP) increased by ~30% over the 20th century (*7*), if carbon uptake efficiency (NPP/GPP) did not change significantly, then NPP should be at least 80 PgC per year presently, but it is only 43 to 76 PgC per year in current models (*5*).

Implications for the carbon cycle

The simulations of ^{14}C that we analyzed provide evidence that CESM2 and most other CMIP6 models underestimate the magnitude of NPP in the 1960s. The minimum NPP of 63 PgC per year in 1965 and 80 PgC per year recently [applying a 30% increase according to (*7*)] that is implied by our analysis of bomb ^{14}C in vegetation is higher than simulated in most CMIP6 models (*5*) (Fig. 2) but within the higher end of the range of observation-based estimates of GPP (*34*–*37*), assuming ~50% NPP/GPP. The global NPP/GPP ratio might increase slightly in the future (*38*), but we are not aware of any evidence for a historical trend. The average NPP in CMIP6 models actually decreased compared with CMIP5 models (*5*, *39*), which likely degraded the model cohort rather than improved it.

Our results highlight parametric and structural uncertainties in model simulations of leaf-level photosynthesis and stomatal conductance, nutrient limitation, autotrophic respiration, carbon allocation, mortality, and turnover. For example, replacing the widely used assumption of homogeneity in wood carbon turnover rates at a given location (*40*) with vegetation demographic models (*41*) that allow distinct populations of fast-growing versus long-lived trees may improve ^{14}C accumulation, where the former are able to rapidly take up ^{14}C whereas the latter dominate the overall biomass pool (*42*). However, because ^{14}C accumulation over 1963 to 1967 is higher in woody than nonwoody vegetation (Fig. 3 and figs. S1 and S4), it is likely that increasing NPP to woody vegetation in models that underestimate ^{14}C accumulation is required. Satisfying observational constraints on carbon stocks while increasing NPP will require that the rate of carbon turnover in the models also increases.

A range of 41 to 64 PgC per year for NPP was found in a previous study using a ^{14}C budget to diagnose the bomb-produced ^{14}C in the biosphere (*9*) and then using this budget to fit parameters in a simple three-box global biosphere model (*43*). Our evaluation of state-of-the-art global biosphere models suggests that the ^{14}C budget in the 1960s cannot be met with NPP lower than 63 PgC per year in current model formulations (Fig. 2B). This is in fact consistent with (*9*), in which the budget was not closed in the 1960s and instead included a residual "hidden sink" that must be in the terrestrial biosphere.

Radiocarbon data provide powerful and unique insights on carbon cycling and model evaluation, but they have been underused because of the low number of models simulating ^{14}C. In addition to the observation-based global ^{14}C accumulation used here and soil carbon ^{14}C data used previously to evaluate CMIP models (*33*, *44*), other data including ^{14}C in specific soil compounds, in respiration, or in atmospheric CO_2 could be used to evaluate more processes in models that simulate ^{14}C. Analyzing the 1963 to 1967 period allowed us to focus on vegetation, but longer analysis of subsequent decades would enable critical insights on whole-ecosystem cycling, including litter and soil (Fig. 1C). Within vegetation alone, ^{14}C simulations strongly diverge over time (Fig. 2A), and there are large differences between models in spatial distribution of ^{14}C accumulation, NPP, and carbon stock (Fig. 4 and fig. S6). Spatial differences in ^{14}C accumulation between models are at least a factor of two but up to a factor of 10 for nonwoody vegetation in northern temperate and boreal regions. Additional ^{14}C data-model comparisons will enable more constraints on various processes. In addition, because we estimated the 1963 to 1967 ^{14}C accumulation in litter and soils based on the CESM-LENS simulations (with ±100% uncertainty), further analysis of ^{14}C through all biospheric pools would help to refine the constraints on vegetation.

The vegetation emulator model that we used here represents the ^{14}C explicitly simulated in CESM2 well (Figs. 2 to 4), but the emulator could not be evaluated for other models, and

emulators for litter and soil pools could not be constructed with the limited variables in the CMIP output. Ensuring an accurate representation of ^{14}C in biospheric models requires that the models explicitly simulate ^{14}C, which only requires one additional tracer to be added in a simple way (*22*). New methods for fast spin-up could be exploited (*45*–*47*). As requested for CMIP6 (*48*), we strongly recommend that modeling groups implement ^{14}C in ESMs and in stand-alone models and report these results to CMIP and related activities to enable model assessment and scientific understanding.

Accurate simulation of vegetation and total biospheric carbon uptake and turnover is critical to understanding historical and future anthropogenic carbon storage in terrestrial ecosystems, both for natural sinks of CO_2 and for "nature-based solutions" that aim to remove atmospheric CO_2 by increasing land ecosystem carbon. Our analysis shows that the uptake of carbon through NPP and the rate of carbon turnover in models must both be increased, which will increase the turnover of anthropogenic carbon in the terrestrial biosphere. Because the uptake and turnover of carbon are the main controls on the anthropogenic CO_2 sink in the terrestrial biosphere, the results of our study suggest that the storage of anthropogenic carbon in the terrestrial biosphere is likely more short-lived and more vulnerable to future changes than previously thought.

REFERENCES AND NOTES

1. P. Friedlingstein *et al*., *Earth Syst. Sci. Data* **15**, 5301–5369 (2023).
2. A. Ito, *Glob. Change Biol.* **17**, 3161–3175 (2011).
3. D. A. Clark *et al*., *Ecol. Appl.* **11**, 356–370 (2001).
4. R. J. Olson, J. M. O. Scurlock, S. D. Prince, D. L. Zheng, K. R. Johnson, "NPP Multi-Biome: Global Primary Data Initiative Produces, R2" (ORNL DAAC, 2013); https://doi.org/10.3334/ORNLDAAC/617.
5. R. M. Varney, S. E. Chadburn, E. J. Burke, P. M. Cox, *Biogeosciences* **19**, 4671–4704 (2022).
6. M. Zhao, F. A. Heinsch, R. R. Nemani, S. W. Running, *Remote Sens. Environ.* **95**, 164–176 (2005).
7. J. E. Campbell *et al*., *Nature* **544**, 84–87 (2017).
8. S. E. Trumbore, *Ecol. Appl.* **10**, 399–411 (2000).
9. T. Naegler, I. Levin, *J. Geophys. Res.* **114**, D17302 (2009).
10. United Nations, "UNSCEAR 2000 report volume 1" (UN Scientific Committee on the Effects of Atomic Radiation, 2000); https://www.unscear.org/unscear/en/publications/2000_1.html.
11. T. Naegler, Simulating bomb radiocarbon: Consequences for the global carbon cycle, PhD Thesis, University of Heidelberg, Heidelberg, Germany (2005).
12. T. Naegler, I. Levin, *J. Geophys. Res.* **111**, D12311 (2006).
13. V. Hesshaimer, I. Levin, *J. Geophys. Res.* **105** (D9), 11641–11658 (2000).
14. H. Graven *et al*., *Geosci. Model Dev.* **10**, 4405–4417 (2017).
15. M. Meinshausen *et al*., *Geosci. Model Dev.* **10**, 2057–2116 (2017).
16. H. D. Graven, N. Gruber, R. Key, S. Khatiwala, X. Giraud, *J. Geophys. Res.* **117**, C10005 (2012).
17. S. Khatiwala, H. Graven, S. Payne, P. Heimbach, *Geophys. Res. Lett.* **45**, 5617–5626 (2018).
18. B. Pookkandy, H. Graven, A. Martin, *Clim. Dyn.* **61**, 3223–3235 (2023).
19. J. G. Lester, Changes in oceanic radiocarbon and CFCs since the 1990s, Zenodo (2023); https://doi.org/10.5281/zenodo.8242144.
20. T. Naegler, *Tellus B Chem. Phys. Meterol.* **61**, 372–384 (2009).
21. S. Peacock, *Global Biogeochem. Cycles* **18**, 2003GB002211 (2004).
22. Materials and methods are available as supplementary materials online.
23. D. M. Lawrence *et al*., *J. Adv. Model. Earth Syst.* **11**, 4245–4287 (2019).
24. CLM5.0 data for: H. D. Graven, H. Warren, H. K. Gibbs, S. Khatiwala, C. Koven, J. Lester, I. Levin, S. A. Spawn-Lee, W. Wieder, Bomb radiocarbon evidence for strong global carbon uptake and turnover in terrestrial vegetation, Climate Data Gateway (2024); https://doi.org/10.5065/d6154fwh.
25. G. Danabasoglu *et al*., *J. Adv. Model. Earth Syst.* **12**, e2019MS001916 (2020).
26. K. B. Rodgers *et al*., *Earth Syst. Dyn.* **12**, 1393–1411 (2021).
27. CESM2-LENS data for: H. D. Graven, H. Warren, H. K. Gibbs, S. Khatiwala, C. Koven, J. Lester, I. Levin, S. A. Spawn-Lee, W. Wieder, Bomb radiocarbon evidence for strong global carbon uptake and turnover in terrestrial vegetation, NCAR Community Earth System Model (2024); https://www.cesm.ucar.edu/community-projects/lens2.
28. T. Frischknecht, A. Ekici, F. Joos, *Global Biogeochem. Cycles* **36**, e2021GB007042 (2022).
29. H. K. Gibbs, A. Ruesch, "New IPCC tier-1 global biomass carbon map for the year 2000" (US Department of Energy, Office of Scientific and Technical Information, 2008); https://www.osti.gov/dataexplorer/biblio/dataset/1463800.
30. S. A. Spawn, C. C. Sullivan, T. J. Lark, H. K. Gibbs, *Sci. Data* **7**, 112 (2020).
31. K.-H. Erb *et al*., *Nature* **553**, 73–76 (2018).
32. P. B. Reich *et al*., *Proc. Natl. Acad. Sci. U.S.A.* **111**, 13721–13726 (2014).
33. Z. Shi *et al*., *Nat. Geosci.* **13**, 555–559 (2020).
34. C. Beer *et al*., *Science* **329**, 834–838 (2010).
35. L. R. Welp *et al*., *Nature* **477**, 579–582 (2011).
36. G. Badgley, L. D. L. Anderegg, J. A. Berry, C. B. Field, *Glob. Chang. Biol.* **25**, 3731–3740 (2019).
37. M.-C. Liang *et al*., *Sci. Rep.* **13**, 2162 (2023).
38. J. M. Mathias, A. T. Trugman, *Ecol. Lett.* **25**, 498–508 (2022).
39. N. Wei *et al*., *J. Clim.* **35**, 5483–5499 (2022).
40. A. Wolf *et al*., *Global Biogeochem. Cycles* **25**, n/a (2011).
41. R. A. Fisher *et al*., *Glob. Chang. Biol.* **24**, 35–54 (2018).
42. J. A. Lutz *et al*., *Glob. Ecol. Biogeogr.* **27**, 849–864 (2018).
43. T. Naegler, I. Levin, *J. Geophys. Res.* **114**, D17303 (2009).
44. Y. He *et al*., *Science* **353**, 1419–1424 (2016).
45. Y. Luo *et al*., *J. Adv. Model. Earth Syst.* **14**, e2022MS003008 (2022).
46. H. Metzler *et al*., *J. Adv. Model. Earth Syst.* **12**, e2019MS001776 (2020).
47. S. Khatiwala, *J. Adv. Model. Earth Syst.* **15**, e2022MS003447 (2023).
48. C. D. Jones *et al*., *Geosci. Model Dev.* **9**, 2853–2880 (2016).
49. CMIP5 and CMIP6 data for: H. D. Graven, H. Warren, H. K. Gibbs, S. Khatiwala, C. Koven, J. Lester, I. Levin, S. A. Spawn-Lee, W. Wieder, Bomb radiocarbon evidence for strong global carbon uptake and turnover in terrestrial vegetation, Earth System Grid Federation (2024); https://esgf-node.llnl.gov/projects/esgf-llnl/.

ACKNOWLEDGMENTS

We dedicate this paper to the memory of Ingeborg Levin, a pioneering, dedicated, and beloved scientist whose ambitions and efforts to measure and use ^{14}C to understand the carbon cycle laid the foundation for this study. We acknowledge the CESM2 Large Ensemble Community Project and supercomputing resources provided by the IBS Center for Climate Physics in South Korea; the World Climate Research Programme, which, through its Working Group on Coupled Modelling, coordinated and promoted CMIP6 and CMIP5; the climate modeling groups for producing and making available their model output; the Earth System Grid Federation (ESGF) for archiving the data and providing access; and the multiple funding agencies who support CMIP6, CMIP5, and ESGF. **Funding:** This work was supported by the Leverhulme Trust, Philip Leverhulme Prize PLP-2018-038; Royal Society Wolfson Fellowship RSWF\FT\191013; Schmidt Sciences, LLC for LEMONTREE (Land Ecosystem Models based On New Theory, obseRvations and ExperimEnts); and by the Office of Science, Office of Biological and Environmental Research of the US Department of Energy under contract DE-AC02-05CH11231 through the Regional and Global Model Analysis (RUBISCO SFA) and Environmental Systems Science (NGEE-Tropics) Programs **Author contributions:** Conceptualization: H.D.G.; Methodology: H.D.G., H.W., C.K., W.W.; Investigation: H.D.G., H.W., H.K.G., S.K., C.K., J.L., I.L., S.S., W.W.; Visualization: H.D.G., J.L.; Writing – original draft: H.D.G.; Writing – review and editing: H.D.G., H.W., H.K.G., S.K., C.K., J.L., I.L., S.S., W.W. **Competing interests:** The authors declare no competing interests. **Data and materials availability:** CMIP5 and CMIP6 model output data are available at (*49*), CLM5.0 data are available at (*24*), and CESM2-LENS data are available at (*26*). Other data are available from references (*10*), (*12*), (*14*–*19*), and (*30*–*32*). All data plotted in the figures are tabulated in data S1 as an Excel spreadsheet.

SUPPLEMENTARY MATERIALS

science.org/doi/10.1126/science.adl4443
Materials and Methods
Figs. S1 to S6
Tables S1 and S2
Data S1

Submitted 18 October 2023; accepted 9 May 2024
10.1126/science.adl4443